Vibration of nonhomogeneous porous Euler nanobeams using boundary characteristics Bernstein Polynomials

R. Selvamani [1*], T. Prabhakaran[2], L. Rubine[2], M. MahaveerSreeJayan[3] and L.Wang[3]

[1, 2] (Department of Mathematics, Karunya Institute of Technology and Sciences, Karunya Nagar, 641114, India)

[3](Mechanical State Key laboratory of Mechanics and Control of Mechanical Structures, Nanjing University of Aeronautics and Astronautics, 210016 Nanjing, People's Republic of china)

*** Corresponding author, Email address: selvam1729@gmail.com**

Abstract:

This study investigates the vibration of non-homogeneous porous Euler nanobeams, incorporating the governing equations of Eringen's nonlocal elasticity theory. To enhance computational efficiency in our analysis, we employ the Rayleigh-Ritz method, harnessing computationally efficient Bernstein polynomials as shape functions. Furthermore, we explore a range of classical boundary conditions tailored to address the specific problem at hand. In order to validate our findings, we conduct a comparative analysis against existing literature, thereby underscoring the effectiveness and robustness of our proposed methodology. Our research also places a significant emphasis on elucidating the impact of scaling parameters, dimensionless amplitude and porosity on dimensionless frequency under various boundary conditions, including Simply-Supported (S-S), Clamped-Simply Supported(C-S), and Clamped-Clamped(C-C) configurations.

Keywords: Euler nanobeam, non-homogeneity, porous nanobeam, Bernstein polynomials, Rayleigh-Ritz method, nonlocal elasticity.

1. Introduction

Accurate prediction of the vibration behavior of non-homogeneous porous Euler nanobeams is essential for advancing various technological fields and ensuring the safety, efficiency and effectiveness of nanoscale devices and systems in real-world applications. Understanding the vibration behavior of non-homogeneous porous nanobeams is essential for designing advanced materials with tailored mechanical properties for specific applications, such as lightweight and high-strength materials for aerospace and automotive industries. In contemporary times, nanomaterials find applications across a multitude of sectors, such as information technology, solar panels, optics, electronics, medical, healthcare applications and more. To achieve the necessary precision in the behavior of nanoresonators (Peng, Chang, Aloni, Yuzvinsky, & Zettl, 2006) and nanoactuators (Dubey et al., 2004), it becomes imperative to account for small-scale effects and atomic forces. Research focusing on nanobeams reveals that conventional beam theories fail to accurately capture the mechanical properties of nanobeams at this scale (Ruud, Jervis, & Spaepan, 1994). Neglecting these small-scale effects can lead to profoundly erroneous solutions in the realm of nano design, resulting in inadequate designs. (Wang & Hu, 2005) demonstrated that classical beam theories are inadequate for predicting the reduction in phase velocities of wave propagation in carbon nanotubes when the wave number is sufficiently high, causing the microstructure to significantly influence the flexural wave dispersion. In response to this challenge, Eringen introduced the nonlocal elasticity theory (Eringen, 1972). Subsequently, (Reddy, 2007) reformulated various beam theories, including Euler-Bernoulli and Timoshenko beam theories, utilizing nonlocal differential constitutive relations. The author derived equations of motion considering these nonlocal theories and furnished corresponding analytical solutions for the bending, buckling and vibration of beams. An analysis was conducted on static and dynamic problems of nanobeams and nanoplates (Chakraverty & Behera, 2016). (Eftekhari & Toghraie, 2022) reported the vibration and dynamic analysis of a cantilever sandwich microbeam integrated with piezoelectric layers, based on strain gradient theory and surface effects. (Hashemian, Falsafioon, Pirmoradian, & Toghraie, 2020) studied the nonlocal dynamic stability analysis of a Timoshenko nanobeam subjected to a sequence of moving nanoparticles, considering surface effects. (Eftekhari, Hashemian, & Toghraie, 2020) discussed optimal vibration control of multi-layer micro-beams actuated by piezoelectric layer based on modified couple stress and surface stress elasticity theories. (Saffari, Hashemian, & Toghraie, 2017) explored the dynamic stability of functionally graded nanobeam based on nonlocal Timoshenko theory considering surface effects.

Nonlocal elasticity theory has found extensive application in the analysis of nanostructures, encompassing nanobeams, nanoplates, nanorings, carbon nanotubes and more. This theory takes into account the forces between atoms and internal length scales (Wang, 2005; Wang, Kitipornchai, Lim, & Eisenberger, 2008; Zhang, Liu, & Xie, 2005). (Karmakar & Chakraverty, 2019) a novel nonlocal beam theory specifically designed for investigating the bending, buckling and free vibration characteristics of nanobeams. Authors (Wang, Zhang, & He, 2007) tackled the problem of free vibration in Euler-Bernoulli nanobeams using analytical methods. In their study, they conducted a comparative analysis of frequency parameters under varying scaling effect parameters and diverse boundary conditions.

Researchers (Phadikar & Pradhan, 2010) employed finite element analysis to solve the equations governing the bending, buckling and vibration behaviour of Euler nanobeams.

Their study encompassed the computation of results for nanobeams subjected to various boundary conditions, including simply supported, clamped and free. In the realm of vibration analysis of nanostructures, different methods have been explored by various researchers. These methods include the finite element method (Eltaher, Emam, & Mahmoud, 2012), the utilization of Chebyshev polynomials within the Rayleigh-Ritz method (Mohammadi & Ghannadpour, 2011), the meshless method (Roque, Ferreira, & Reddy, 2011).Vibration properties of functionally graded nano-plates were examined using a novel nonlocal refined four-variable model (Belkorissat, Houari, Tounsi, Bedia, & Mahmoud, 2015). Later, a nonlocal zeroth-order shear deformation theory was presented for the free vibration of functionally graded nanoscale plates resting on an elastic foundation (Bounouara, Benrahou, Belkorissat, & Tounsi, 2016). (Pradhan & Murmu, 2010) the application of nonlocal elasticity and Differential Quadrature Method (DQM) in the flapwise bending vibration of rotating nano cantilevers was discussed.

The functional and structural significance of poroelastic materials is leading to significant advancements in geological, biological and synthetic fields. These porous materials find extensive applications in aerospace and construction models due to their low relative density, high surface area, amplified specific strength, lightweight nature, thermal insulation properties and good permeability. Analyzing nonlinear vibrations of metal foam nanobeams with symmetric and non-symmetric porosities was discussed by (Alasadi, Ahmed, & Faleh, 2019). Effect of thickness stretching and porosity on mechanical response of a functionally graded beams resting on elastic foundations was discussed in detail (Atmane, Tounsi, Bernard, & Mahmoud, 2015a, 2015b) a computational shear displacement model for vibrational analysis of functionally graded beams with porosities has been introduced. (Behera & Chakraverty, 2014) discussed the free vibration of Euler and Timoshenko nanobeams using boundary characteristic orthogonal polynomial. In a separate study, (Barati, 2017a, 2017b) conducted research on nonlocal-strain gradient forced vibration analysis of metal foam nanoplates with uniform and graded porosities. Furthermore, in another investigation, explored the vibration analysis of Functionally Graded (FG) nanoplates with nanovoids on a viscoelastic substrate under hygro-thermo-mechanical loading using nonlocal strain gradient theory. The effect of porosity on the free and forced vibration characteristics of the Graphene Platelet (GPL) reinforcement composite nanostructures was explored (Pourjabari, Hajilak, Mohammadi, Habibi, & Safarpour, 2019). Research conducted on the size-dependent bending and vibration behaviour of piezoelectric nanobeams due to flexoelectricity (Yan & Jiang, 2013).

(Civalek, Ersoy, Uzun, & Yaylı, 2023) explored the dynamics of microbeams composed of functionally graded porous material with metal foam, taking into account deformable boundaries. The impact of porosity on the dynamic response of arbitrary restrained functionally graded nanobeams was investigated by (Uzun & Yaylı, 2023) using the Modified Couple Stress Theory (MCST). In a separate study, (Civalek, Uzun, & Yaylı, 2023) focused on the nonlinear stability analysis of saturated embedded porous nanobeams. Additionally, (Uzun & Yaylı, 2022) studied the torsional vibrations of restrained functionally graded nanotubes, considering porosity and employing the modified couple stress theory. Lastly, (Uzun & Yaylı, 2023) examined the effects of porosity and deformable boundaries on the dynamics of nonlocal sigmoid and power-law functionally graded nanobeams embedded in the Winkler–Pasternak medium. A comprehensive investigation into the mechanical behavior of functionally graded porous nanobeams resting on an elastic foundation was conducted by (Enayat, Hashemian, Toghraie, & Jaberzadeh, 2020). Free vibration analysis of microtubules as cytoskeleton components was explored (Civalek & Akgoz, 2010). Discussions focused on free and forced vibrations of shear deformable functionally graded porous beams (Chen, Yang, & Kitipornchai, 2016). (Ebrahimi & Daman 2017)The dynamic characteristics of curved inhomogeneous nonlocal porous beams in a thermal environment were examined. The dynamic response of porous inhomogeneous nanobeams on a hybrid Kerr foundation under hygro-thermal loading was studied (Barati, 2017).

In this study, the elastic waves of non-homogeneous porous Euler nanobeams are derived analytically through different boundary conditions. The authentication of present study is done via comparison with existing literature and found a very good agreement. Moreover, this computational approach requires less time compared to prior methods employing Bernstein polynomials. In this context, we have utilized Simple Bernstein Polynomials (SBPs), and additionally, we have subjected the SBPs to orthogonalization via the Gram-Schmidt process to acquire Orthogonal Bernstein Polynomials (OBPs). For a particular example of the present model, the numerical values of the scaling parameters, dimensionless amplitude, and porosity are computed and graphically illustrated to visualize the effects of dimensionless frequency and various boundary conditions.

2. Modeling of porous metal nanobeam

The metal's material traits are contingent upon the distribution of voids or pores. These voids can be distributed uniformly or in non-uniform patterns. In cases of non-uniform distribution, it can be further categorized as symmetric (non-uniform 1) or asymmetric (non-uniform 2). Subsequently, the forthcoming section will introduce the expressions for the material properties, specifically the elastic modulus (E) and mass density(ρ), pertaining to metal foam.

$$E = E_2(1 - e_0 X), \rho = \rho_2\sqrt{(1 - e_0 X)}$$

$$X = \frac{1}{e_0} - \frac{1}{e_0}\left(\frac{2}{\pi}\sqrt{1 - e_0} - \frac{2}{\pi} + 1\right)^2 \text{Uniform} \tag{1}$$

$$E(z) = E_2\left(1 - e_0\cos\left(\frac{\pi z}{h}\right)\right), \rho(z) = \rho_2\left(1 - e_m\cos\left(\frac{\pi z}{h}\right)\right) \text{Non-uniform1} \tag{2}$$

$$E(z) = E_2\left(1 - e_0\cos\left(\frac{\pi z}{2h} + \frac{\pi}{4}\right)\right), \rho(z) = \rho_2\left(1 - e_m\cos\left(\frac{\pi z}{h} + \frac{\pi}{4}\right)\right) \text{Non-uniform 2} \tag{3}$$

In above definitions, the index 2 refers to a material property at its highest value. Also, there are two coefficients e_0 and e_m elated to pore amount and mass distribution as

$$e_0 = 1 - \frac{E_2}{E_1} = 1 - \frac{G_2}{G_1}, e_m = 1 - \sqrt{1 - e_0} \tag{4}$$

2.1 Bernstein Polynomials (BPs)

Bernstein polynomials play a crucial role in numerical techniques for addressing differential equations or systems of equations. They serve as fundamental functions in approaches such as collocation methods or Rayleigh-Ritz, wherein the equations undergo transformation into a set of algebraic equations for numerical resolution.In this section, we delineate the essential features of Bernstein polynomials. A grasp of these pivotal attributes will enable us to address the non-homogeneous nonlinear integro-differential equation (29). Bernstein polynomials of degree n, defined over the interval [0, 1], are formally articulated as follows:

$$B_{i,n}(X) = \binom{n}{i} X^i (1 - X)^{n-i} \quad i = 0,1,\dots n x \in [0,1] \tag{5}$$

In which coefficients

$\binom{n}{i} = \frac{n!}{i!(n-i)!}$. Typically, Bernstein polynomials come in degrees up to n. Specific instances of Bernstein polynomials include

$$B_{1,0}(x) = 1 - x, B_{1,1}(x) = x \tag{6}$$

$$B_{2,0}(x) = (1 - x)^2, B_{2,1}(x) = 2x(1 - x), B_{2,2}(x) = x^2 \tag{7}$$

$$B_{3,0}(x) = (1 - x)^3, B_{3,1}(x) = 3x(1 - x)^2, B_{3,2}(x) = 3x^2(1 - x), B_{3,3}(x) = x^3 \tag{8}$$

2.2 Characteristics of Bernstein Polynomials (BPs)

(i) Partition of unity: In the context of Bernstein polynomials, the partition of unity property states that for any arbitrary value of x in the interval [0, 1], the sum of n+1 Bernstein polynomials of degree n equals one.

$$\sum_0^n B_{n,i}(x) = 1 \tag{9}$$

(ii) Interval end conditions: The interval end conditions for Bernstein polynomials typically involve specifying the values of the polynomial at the endpoints of the interval. There are different types of end conditions depending on the specific requirements of the problem being solved. Two common types of end conditions are:

$$B_{n,i}(0) = \begin{cases} 1 & if i = 0 \\ 0 & if i \neq 0 \end{cases}, \quad B_{n,i}(1) = \begin{cases} 1 & if i = n \\ 0 & if i \neq n \end{cases} \tag{10}$$

(iii) Symmetry: The Bernstein polynomials of even degree n are symmetric about the midpoint of the interval [0, 1] which is x=0.5. Mathematically, this symmetry can be expressed as:

$$B_{n,i}(x) = B_{n,n-i}(1 - x) \tag{11}$$

(iv) Recurrence formula: The recurrence formula in the context of Bernstein polynomials is a key concept used to compute Bernstein polynomials of degree n by blending together two Bernstein polynomials of degree n−1.

$$B_{n,i}(x) = (1 - x)B_{n-1,i}(x) + xB_{n-1,i-1}(x) \tag{12}$$

(v) Derivatives: Using the definition of BPs, equation (5), the first derivative of nth-degree BPs can be written as a linear combination of BPs with degree n – 1

$$\frac{d}{dx} B_{n,i}(x) = n(B_{n-1,i-1}(x) - B_{n-1,i}(x)) \tag{13}$$

(vi) Integration: The integral of a Bernstein polynomial $B_{n,i}(x)$ of degree n over the interval [0, 1] can be computed using the following formula:

$$\int_0^1 B_{n,i}(x) = \frac{1}{n+1} \tag{14}$$

3. Formulation of the problem

The expression defining the strain-displacement relationship according to Euler-Bernoulli beam theory is expressed as:

$$\varepsilon_{xx} = -z \frac{d^2 x}{dx^2} \tag{15}$$

in which x represents the longitudinal coordinate from the left end of the beam, ε_{xx} denotes the normal strain. Z indicates the coordinate measured from the beam's midsection, while ω signifies the transverse displacement. Let's denote the strain energy as U, as defined by (Behera & Chakraverty, 2014)

$$U = \frac{1}{2} \int_0^L \int_A \sigma_{xx} \varepsilon_{xx} dA dx \tag{16}$$

in this context, σ_{xx} represents the normal stress, A denotes the cross-sectional area of the beam, and L stands for the beam's length. The bending moment is expressed as:

$$M = \int_A \sigma_{xx} z dA. \tag{17}$$

By employing Equations (15) and (17) within Equation (16), the maximum strain energy can be articulated as:

$$U_{max} = -\frac{1}{2} \int_0^L M \frac{d^2 w}{dx^2} dx. \tag{18}$$

Presuming unrestricted harmonic motion, the maximum kinetic energy is derived as:

$$T_{max} = \frac{1}{2}\int_0^L \rho A \omega^2 w^2 dx \tag{19}$$

where ω represents the circular frequency of the vibration, and ρ signifies the mass density of the beam material. The governing equation of motion, excluding rotary inertia, is described by (Civalek & Akgoz, 2010)

$$\frac{d^2 M}{dx^2} = -\rho A \omega^2 w. \tag{20}$$

For an elastic material in the one-dimensional case, Eringen's nonlocal constitutive relation may be written as (Karmakar & Chakraverty, 2019)

$$\sigma_{xx} - (e_0 a)^2 \frac{d^2 \sigma_{xx}}{dx^2} = E\varepsilon_{xx} \tag{21}$$

here, E represents Young's modulus, with $e_0 a$ denoting the scale coefficient encompassing the small-scale effect. The parameter 'a' represents the internal characteristic length, for instance, the lattice parameter, C-C bond length, or granular distance. Meanwhile, e_0 stands as a constant specific to each material. Determining the value of e_0 might involve experimental measures or an approximation obtained by aligning the dispersion curves of plane waves with those of atomic lattice dynamics.

Now multiplying equation (21) by zdA and integrating over the area A, we can get the following relation

$$M - (e_0 a)^2 \frac{d^2 M}{dx^2} = -EI\frac{d^2 w}{dx^2} \tag{22}$$

where I is the second moment of inertia.

4. Nonhomogeneous case

In this section we consider the non-homogeneous Euler nanobeam. Firstly the Young's modulus and density varies linearly with respect to x; $E = E_0(1 + \alpha x)$ and

$\rho = \rho_0(1+\beta x)$ (Behera & Chakraverty, 2014). Then after putting the above expressions of E and ρ, the equation (22) is rewritten as

$$M = -E_0(1+\alpha x)I\frac{d^2 w}{dx^2} - (e_0 a)^2 \rho_0 (1+\beta x)A\omega^2 w \tag{23}$$

5. Solution methodology

The vibration equation of the Euler nanobeam has been solved using the Rayleigh-Ritz method, utilizing Bernstein polynomials as the fundamental basis function. To aid in this process, we introduce the following non-dimensional terms:

$$X = \frac{x}{L}$$

$$W = \frac{w}{L}$$

$\varsigma = \frac{e_0 a}{L}$ is scaling effect parameter.

5.1 Bernstein based Rayleigh-Ritz method

The displacement W is designed as

$$W(X) = \sum_{i=0}^{n} c_i \phi_i \tag{24}$$

where c_i's are the unknown constants and n is the order of the approximation.

The shape function ϕ_i's are chosen as

$$\phi_i(X) = \eta_b B_{i,n}(X) \tag{25}$$

where $B_{i,n}(X)$ indicates the Bernstein polynomials (Chakraverty & Behera, 2016)

$$B_{i,n}(X) = \binom{n}{i} X^i (1-X)^{n-i} \tag{26}$$

here $\binom{n}{i} = \frac{n!}{i!(n-i)!}$; $i = 0,1,\dots n$ and η_b is the dimensionless boundary polynomial in various nanobeam boundary conditions which is considered as,

$$\eta_b = X^p (1-X)^q \tag{27}$$

here, the variables p and q assume values of 0, 1, or 2, corresponding to free, simply supported, or clamped boundary conditions, respectively. Consequently, we can readily address the problem's boundary conditions by utilizing different combinations of p and q. Within the Rayleigh–Ritz method, we can take the following relation:

$$U_{max} = T_{max} \tag{28}$$

By substituting Equation (24) into Equation (28) and performing partial differentiation with respect to the unknown c_i's, we arrive at a generalized Eigenvalue problem formulated as:

$$[P]\{Y\} = \lambda^2 [M]\{Y\} \tag{29}$$

where, $\lambda^2 = \frac{\rho_0 A \omega^2 L^4}{E_0 L}$ is frequency parameter, $\{Y\}=[c_0 c_1 .... c_n]^T$, $\alpha_i = (1+\alpha XL), \beta_i = (1+\beta XL)$ and the matrices M and P are the mass and stiffness matrices respectively, which are given below

$$P = \begin{bmatrix} \int_0^1 \phi_0'' \phi_0'' dX & \int_0^1 \phi_1'' \phi_0'' dX \ldots & \int_0^1 \phi_n'' \phi_0'' dX \\ \int_0^1 \phi_0'' \phi_1'' dX & \int_0^1 \phi_1'' \phi_1'' dX \ldots & \int_0^1 \phi_n'' \phi_1'' dX \\ .. & .. & .. \\ \int_0^1 \phi_0'' \phi_n'' dX & \int_0^1 \phi_1'' \phi_n'' dX \ldots & \int_0^1 \phi_n'' \phi_n'' dX \end{bmatrix}$$

$$M = \begin{bmatrix} \int_0^1 \frac{\beta_i}{\alpha_i}(\phi_0 \phi_0 - \frac{a^2}{2}\phi_0 \phi_1'' - \frac{a^2}{2}\phi_0'' \phi_1) dX & \int_0^1 \frac{\beta_i}{\alpha_i}(\phi_1 \phi_0 - \frac{a^2}{2}\phi_1 \phi_0'' - \frac{a^2}{2}\phi_1'' \phi_0) dX \ldots & \int_0^1 \frac{\beta_i}{\alpha_i}(\phi_n \phi_0 - \frac{a^2}{2}\phi_n \phi_0'' - \frac{a^2}{2}\phi_n'' \phi_0) dX \\ \int_0^1 \frac{\beta_i}{\alpha_i}(\phi_0 \phi_1 - \frac{a^2}{2}\phi_0 \phi_1'' - \frac{a^2}{2}\phi_0'' \phi_1) dX & \int_0^1 \frac{\beta_i}{\alpha_i}(\phi_1 \phi_1 - \frac{a^2}{2}\phi_1 \phi_1'' - \frac{a^2}{2}\phi_1'' \phi_1) dX \ldots & \int_0^1 \frac{\beta_i}{\alpha_i}(\phi_n \phi_1 - \frac{a^2}{2}\phi_n \phi_1'' - \frac{a^2}{2}\phi_n'' \phi_1) dX \\ .. & .. & .. \\ \int_0 \frac{\beta_i}{\alpha_i}(\phi_0 \phi_n - \frac{a^2}{2}\phi_0 \phi_n'' - \frac{a^2}{2}\phi_0'' \phi_n) dX & \int_0^1 \frac{\beta_i}{\alpha_i}(\phi_1 \phi_n - \frac{a^2}{2}\phi_1 \phi_n'' - \frac{a^2}{2}\phi_1'' \phi_n) dX \ldots & \int_0^1 \frac{\beta_i}{\alpha_i}(\phi_n \phi_n - \frac{a^2}{2}\phi_n \phi_n'' - \frac{a^2}{2}\phi_n'' \phi_n) dX \end{bmatrix}$$

where $\phi_i'' = \frac{d^2}{dx^2}(B_{i,n}(X).\eta_b(X))$

5.2 Solution using Orthogonal Bernstein Polynomials (OBPs)

We express the displacement function as

$$W(X) = \sum_{i=0}^{n} c_i \hat{\Phi}_i \quad (30)$$

where $\hat{\Phi}_i$'s are Orthogonal Bernstein Polynomials, which are taken via Gram-Schmidt orthogonalizations follows

$$\theta_i = \eta_b B_{i,n}(X)$$

where $B_{i,n}(X)$, η_b are defined in equations (22) and (23), respectively.

$$\hat{\Phi}_0 = \theta_0$$

$$\hat{\Phi}_i = \theta_i - \sum_{j=0}^{i-1} \beta_{ij} \hat{\Phi}_j \quad (31)$$

where $\beta_{ij} = \frac{<\theta_i, \theta_j>}{<\hat{\Phi}_j, \hat{\Phi}_j>}$

here the inner product <,> is defined as $< \hat{\Phi}_j, \hat{\Phi}_j >= \int_0^1 \hat{\Phi}_i(X), \hat{\Phi}_j(X) dX$, and the norm can be written as

$$||\hat{\Phi}_i|| =< \hat{\Phi}_i, \hat{\Phi}_j >^{1/2} = [\int_0^1 \hat{\Phi}_i(X) \hat{\Phi}_i(X) dX]^{1/2} \quad (32)$$

We assert that the presumed displacement function in Equation (24) will converge concerning the specified shape functions, namely Bernstein polynomials (defined in Equation (26)).

6. Numerical results and discussion

After the derivation of closed form vibration frequency of porous non-homogeneous nanobeams shown in Figure1, it is possible to find its dependency on various factors including scaling parameter, porosity pattern and nonlocal effects. To do this, a set of material constants are taken (Alasadi et al., 2019) as E_2 =200 GPa ρ_2=7850 kg/m^3, ν=0.33, I = $\pi d^4/64$ and L=10h.Void or pore dispersion is set as uniform and non-uniform with different values for its coefficient. The vibration frequency of a large size beam might be achieved by selecting a zero nonlocal parameter.

Tables 1 and 2 exhibits the numerical results for the non-dimensionless frequencies computed by using BPs and OBPs method, respectively for various non-homogeneous and nonlocal values. From these tables it is observed that the frequencies are increasing for increasing non-homogeneous values and condensed for increasing nonlocal values. That leads to the conclusion that. Also, the BPs method getting higher values compared with OBPs method. It is worthy to note that, for linearly varying E and ρ, frequencies amplifies with respect to α and condensed with respect to β. In table 3, first four frequency parameters of Euler–Bernoulli nanobeams are presented for different end conditions and scaling effect parameters. Present results are compared with results of (Wang et al., 2007) and are found to be in good agreement. Frequency parameters for local Euler–Bernoulli nanobeams are also incorporated in this table. Variation of non-dimensional frequency over scaling effect parameter for different modes and various boundary conditions are presented in Figures 3-5. The analysis of Figures 3 to 5 indicates a consistent trend: as scaling effect parameters increase, the frequency parameters exhibit a decreasing pattern. However, a noteworthy observation emerges regarding the increased deflection associated with scaling effects for higher modes under various boundary conditions. This phenomenon suggests that as the system experiences greater scaling effects, it tends to exhibit greater flexibility or deformation, particularly noticeable in higher vibration modes across different boundary conditions. This insight highlights the intricate relationship between scaling effects and structural behavior, shedding light on the mechanical response of the system. Figures 6-8 display the dispersion of non-dimensional frequency over non-dimensional amplitudes for different porous pattern and various boundary conditions. Examining Figures 6-8 reveals that the non-dimensional frequency undergoes heightened variation with an increase in non-dimensional amplitude, with particularly enhanced values along the C-C edge. Notably, the observations indicate that a nano-sized beam characterized by nano porous type 2 exhibits the highest vibration frequency. In contrast, the curves for uniform nano porous and nano porous type 1 closely align. These trends suggest that a nano sized beam featuring a symmetrical void type may achieve superior beam stiffness and overall outstanding mechanical properties. This interpretation underscores the significant impact of nano structural characteristics on the dynamic behavior and mechanical performance of the beam.

7. Conclusions

This study investigates the vibration behavior of non-homogeneous porous Euler nanobeams using equations derived from Eringen's nonlocal elasticity theory. We streamline computational efficiency by applying the Bernstein polynomials based Rayleigh-Ritz method. To verify our results, we compare them with existing literature, demonstrating the effectiveness and reliability of our approach. Our research also emphasizes understanding the influence of scaling parameters, dimensionless amplitude, and porosity on dimensionless frequency under different boundary conditions. Based on our findings, the following key points are highlighted.

- The dimensionless frequency decreases as scaling effect parameters increase, and higher vibration modes exhibit amplified magnitudes.
- Non-homogeneous parameters exert a significant influence on frequency parameters.

- The dimensionless frequency parameters of clamped nanobeams increase with physical variables.
- Nanoscale beams characterized by nano porous type 2 exhibit the highest vibration frequencies.
- An observation of softening behavior is noted for amplified values of nonlocal parameters.
- These results contribute to a deeper understanding of the dynamic response of non-homogeneous porous nanobeams, highlighting the intricate interplay between various physical parameters and vibration characteristics.

References

Alasadi, A. A., Ahmed, R. A., & Faleh, N. M. (2019). Analyzing nonlinear vibrations of metal foam nanobeams with symmetric and non-symmetric porosities. *Advances in Aircraft and Spacecraft Science*, 6(4), 273-282.

Atmane, H.A., Tounsi, A., & Bernard, F. (2015a). Effect of thickness stretching and porosity on mechanical response of a functionally graded beams resting on elastic foundations. *International Journal of Mechanical and Materials in Design*, 13(1), 71-84.

Atmane, H. A., Tounsi, A., Bernard, F., & Mahmoud, S. R. (2015b). A computational shear displacement model for vibrational analysis of functionally graded beams with porosities. *Steel Composite Structures*, 19(2), 369-384.

Barati, M. R. (2017). Investigating dynamic response of porous inhomogeneous nanobeams on hybrid Kerr foundation under hygro-thermal loading. *Applied Physics A*, 123(5), 332.

Barati, M. R. (2017a). Nonlocal-strain gradient forced vibration analysis of metal foam nanoplates with uniform and graded porosities. *Advances in Nano Research*, 5(4), 393-414.

Barati, M. R. (2017b). Vibration analysis of FG nanoplates with nanovoids on viscoelastic substrate under hygro-thermo-mechanical loading using nonlocal strain gradient theory. *Structural Engineering and Mechanics*, 64(6), 683- 693.

Behera, L., & Chakraverty, S. (2014). Free vibration of Euler and Timoshenko nanobeams using boundary characteristic orthogonal polynomial. *Applied nanoscience*, (4), 347–358.

Belkorissat, I., Houari, M. S. A., Tounsi, A., Bedia, E.A., & Mahmoud, S.R. (2015). On vibration properties of functionally graded nano-plate using a new nonlocal refined four variable model. *Steel Composite structures*, 18(4), 1063-1081.

Bounouara, F., Benrahou, K. H., Belkorissat, I., & Tounsi, A. (2016). A nonlocal zeroth-order shear deformation theory for free vibration of functionally graded nanoscale plates resting on elastic foundation. *Steel and Composite Structure*, 20(2), 227-249.

Chakraverty, S., & Behera, L. (2016). Static and Dynamic Problems of Nanobeams and Nanoplates. *World Scientific*.

Chen, D., Yang, J., & Kitipornchai, S. (2016). Free and forced vibrations of shear deformable functionally graded porous beams. *International journal of mechanical sciences*, 108, 14-22.

Civalek, O., & Akgoz, B. (2010). Free vibration analysis of microtubules as cytoskeleton components: Nonlocal Euler–Bernoulli beam modeling. *Iranian Journal of Science and Technology*, 17, 367–375.

Civalek, Ö., Ersoy, H., Uzun, B., & Yaylı, M. Ö. (2023). Dynamics of a FG porous microbeam with metal foam under deformable boundaries. *Acta Mechanica*, 234(11), 5385-5404.

Civalek, Ö., Uzun, B., & Yaylı, M. Ö. (2023). On nonlinear stability analysis of saturated embedded porous nanobeams. *International Journal of Engineering Science*, 190, 103898.

Dubey, A., Sharma, G., Mavroidis, C., Tomassone, M. S., Nikitczuk, K., & Yarmush, M. L. (2004). Computational studies of viral protein nano-actuators. *Journal of Computational and Theoretical Nanoscience,* 1, 18–28.

Ebrahimi, F., & Daman, M. (2017). Dynamic characteristics of curved inhomogeneous nonlocal porous beams in thermal environment. *Structural Engineering and Mechanics*, *64*(1), 121-133.

Eftekhari, S. A., & Toghraie, D. (2022). Vibration and dynamic analysis of a cantilever sandwich microbeam integrated with piezoelectric layers based on strain gradient theory and surface effects. Applied Mathematics and Computation, 419, 126867.

Eftekhari, S. A., Hashemian, M., & Toghraie, D. (2020). Optimal vibration control of multi-layer micro-beams actuated by piezoelectric layer based on modified couple stress and surface stress elasticity theories. Physica A: Statistical Mechanics and its Applications, 546, 123998.

Eltaher, M. A., Emam, S. A., & Mahmoud, F. F. (2012). Free vibration analysis of functionally graded size-dependent nanobeams. *Applied Mathematics and Computation*, 218, 7406–7420.

Enayat, S., Hashemian, M., Toghraie, D., & Jaberzadeh, E. (2020). A comprehensive study for mechanical behavior of functionally graded porous nanobeams resting on elastic foundation. *Journal of the Brazilian Society of Mechanical Sciences and Engineering*, 42, 1-24.

Eringen, A.C. (1972). Nonlocal polar elastic continua. *International Journal of Engineering Science*, 10, 1–16.

Hashemian, M., Falsafioon, M., Pirmoradian, M., & Toghraie, D. (2020). Nonlocal dynamic stability analysis of a Timoshenko nanobeam subjected to a sequence of moving nanoparticles considering surface effects. *Mechanics of Materials*, 148, 103452.

Karmakar, S., & Chakraverty, S. (2019). Boundary Characteristic Bernstein Polynomials Based Solution for Free Vibration of Euler Nanobeams. *Journal of composites Science*, 3(4), 99.

Mohammadi, B., & Ghannadpour, S.A.M. (2011). Energy approach vibration analysis of nonlocal Timoshenko beam theory. *Procedia Engineering*, 10, 1766–1771.

Peng, H. B., Chang, C.W., Aloni, S., Yuzvinsky, T.D., & Zettl, A. (2006). Ultrahigh frequency nanotube resonators. *Physical Review Letters*, 97, 087203.

Phadikar, J. K., & Pradhan, S. C. (2010). Variational formulation and finite element analysis for nonlocal elastic nanobeams and nanoplates. *Computational materials science*, 49, 492–499.

Pourjabari, A., Hajilak, Z. E., Mohammadi, A., Habibi, M., & Safarpour, H. (2019). Effect of porosity on free and forced vibration characteristics of the GPL reinforcement composite nanostructures. *Computers & Mathematics with Applications*, 77(10), 2608-2626.

Pradhan, S. C., & Murmu, T. (2010). Application of nonlocal elasticity and DQM in the flapwisebending vibration of rotating nanocantilever. *Physica E: Low-dimensional systems and nanostructures*, 42, 1944–1949.

Reddy, J. N. (2007). Nonlocal theories for bending, buckling and vibration of beams. *International Journal of Engineering Science*, 45, 288–307.

Roque, C.M.C., Ferreira, A.J.M., & Reddy, J.N. (2011). Analysis of Timoshenko nanobeamswith a nonlocal formulation and meshless method. *International Journal of Engineering Science*, 49, 976–984.

Ruud, J. A., Jervis, T. R., & Spaepan, F. (1994). Nanoindentation of Ag/Ni multi-layered thin films. *Journal of Applied Physics*, 75, 4969.

Saffari, S., Hashemian, M., & Toghraie, D. (2017). Dynamic stability of functionally graded nanobeam based on nonlocal Timoshenko theory considering surface effects. Physica B: Condensed Matter, 520, 97-105.

Uzun, B., & Yaylı, M. Ö. (2023). Porosity effects on the dynamic response of arbitrary restrained FG nanobeam based on the MCST. *Zeitschrift für Naturforschung A*, (0).

Uzun, B., & Yaylı, M. Ö. (2022). Porosity dependent torsional vibrations of restrained FG nanotubes using modified couple stress theory. *Materials Today Communications*, *32*, 103969.

Uzun, B., & Yayli, M. Ö. (2023). Porosity and Deformable Boundary Effects on the Dynamic of Nonlocal Sigmoid and Power-Law FG Nanobeams Embedded in the Winkler–Pasternak Medium. *Journal of Vibration Engineering & Technologies*, 1-20.

Wang, C.M., Kitipornchai, S., Lim, C.W., & Eisenberger, M. (2008). Beam bending solution based on nonlocal Timoshenko beam theory. *Journal of Engineering Mechanics*, 134, 475–481.

Wang, Q. (2005). Wave propagation in carbon nanotubes via nonlocal continuum mechanics. *Journal of Applied Physics*, 98, 124301.

Wang, C. M., Zhang, Y.Y., & He, X.Q. (2007). Vibration of nonlocal Timoshenko beams. *Institute of Physics*, 18, 105401.

Wang, L. F., & Hu, H.Y. (2005). Flexural wave propagation in single-walled carbon Nanotubes. *Physical Review B*, 71, 195412.

Yan, Z., & Jiang, L. (2013). Size-dependent bending and vibration behaviour of piezoelectric nanobeams due to flexoelectricity. *Journal of Physics D: Applied Physics*, *46*(35), 355502.

Zhang, Y. Q., Liu, G. R., & Xie, X. Y. (2005). Free transverse vibrations of double-walled carbon nanotubes using a theory of nonlocal elasticity. *Physical Review Applied*, B 71, 195404.

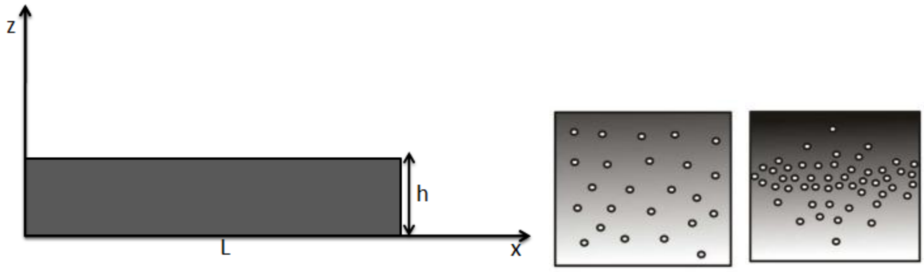

(a) (b) (c)

Figure 1 (a) Geometry of porous nanobeam. (a) Uniform porous nanobeam (b) Non-uniform porous beam

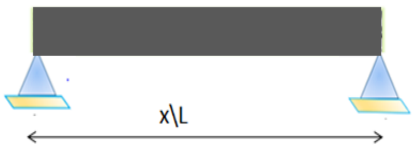

(a)

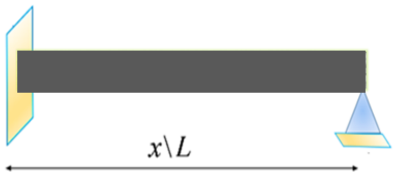

(b)

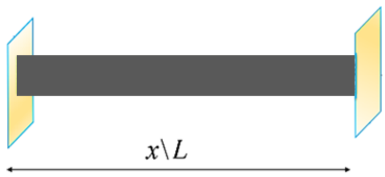

(c)

Figure 2 Boundary conditions. (a) S-S (b) C-S (c) C-C

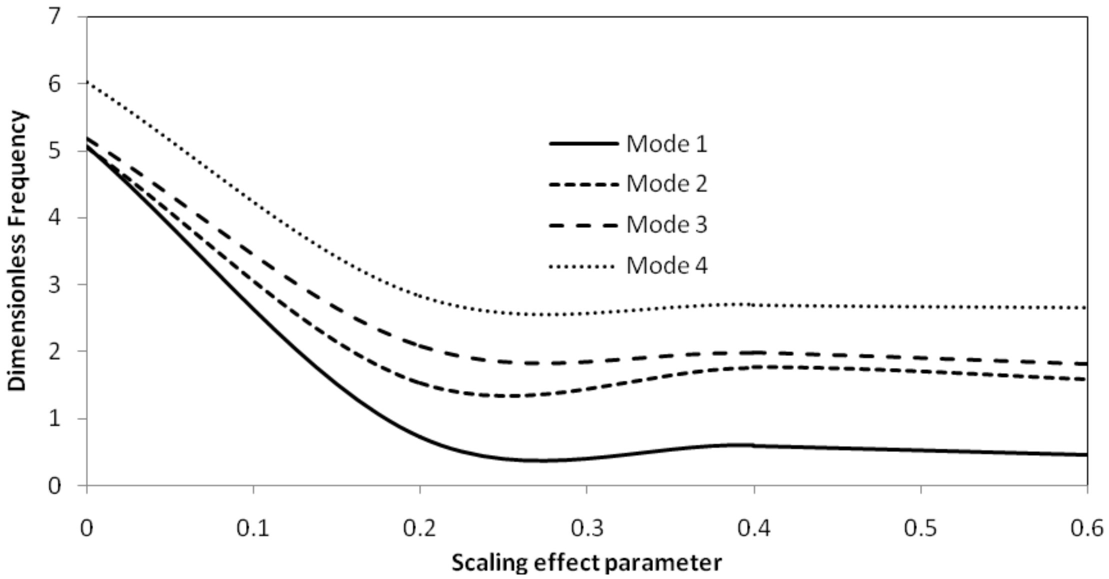

Figure 3 Changes in frequency parameters over scaling effects for S-S boundary conditions.

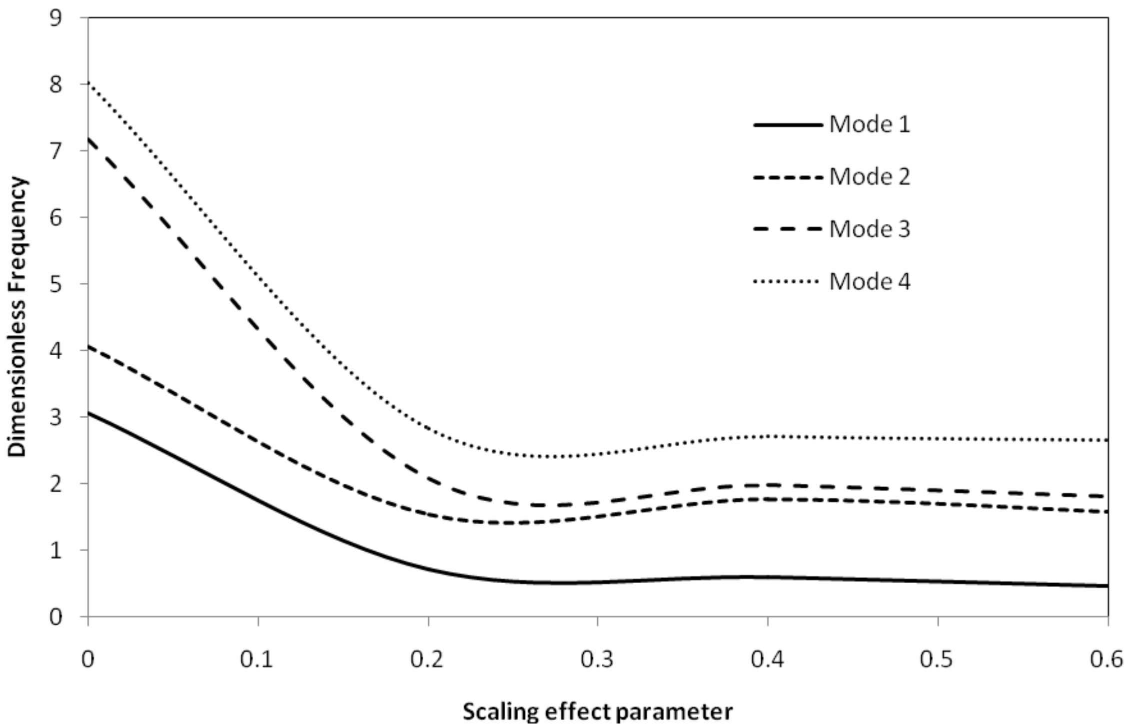

Figure 4 Changes in frequency parameters over scaling effects for C-S boundary.

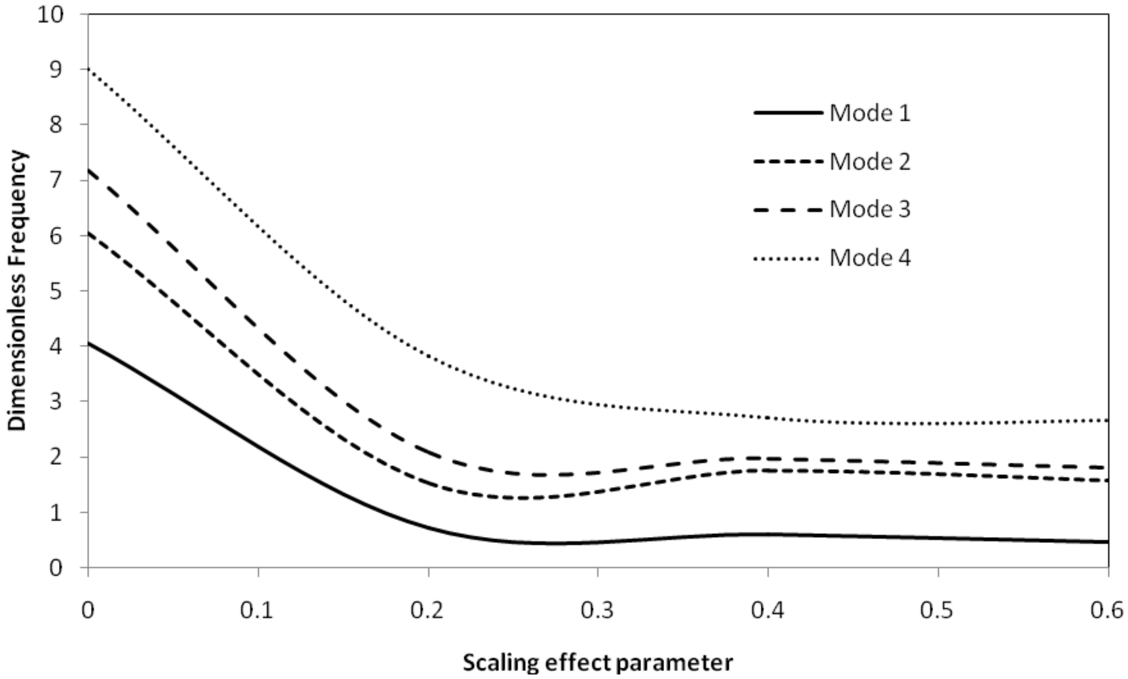

Figure 5 Changes in frequency parameters over scaling effects for C-C boundary.

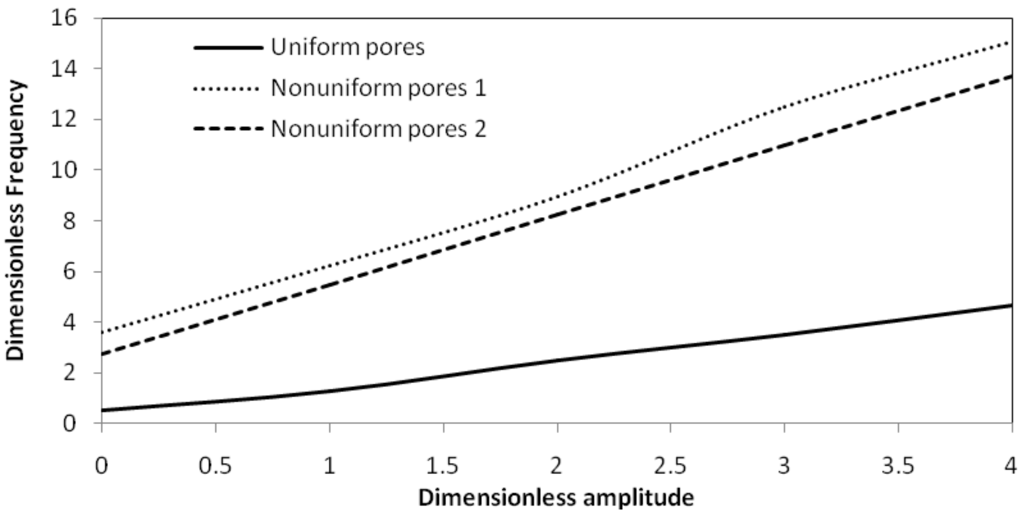

Figure 6 Changes in dimensionless amplitude over dimensionless frequency for S-S boundary.

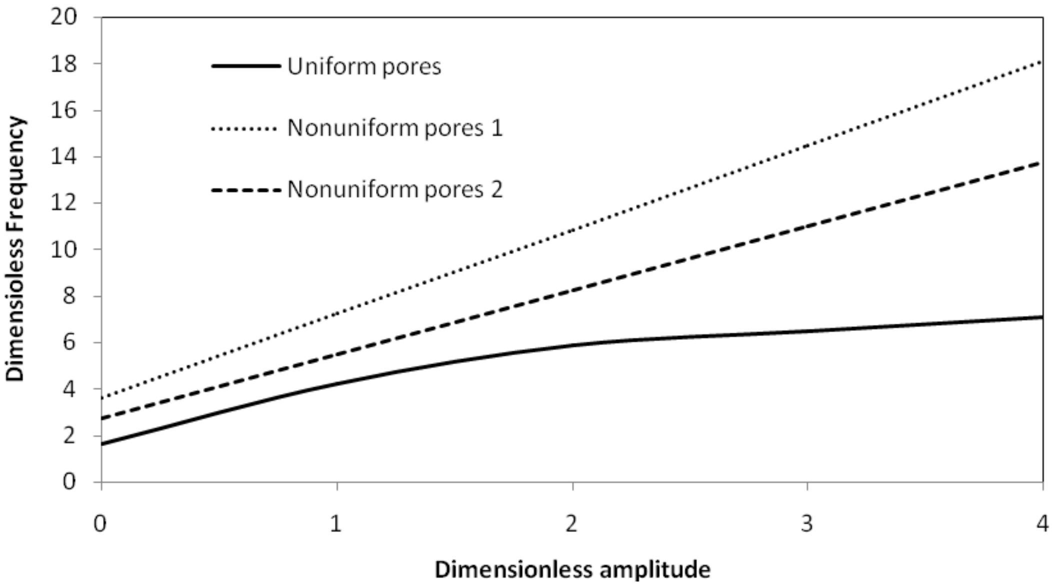

Figure 7 Changes in dimensionless frequency over dimensionless amplitude for C-S boundary.

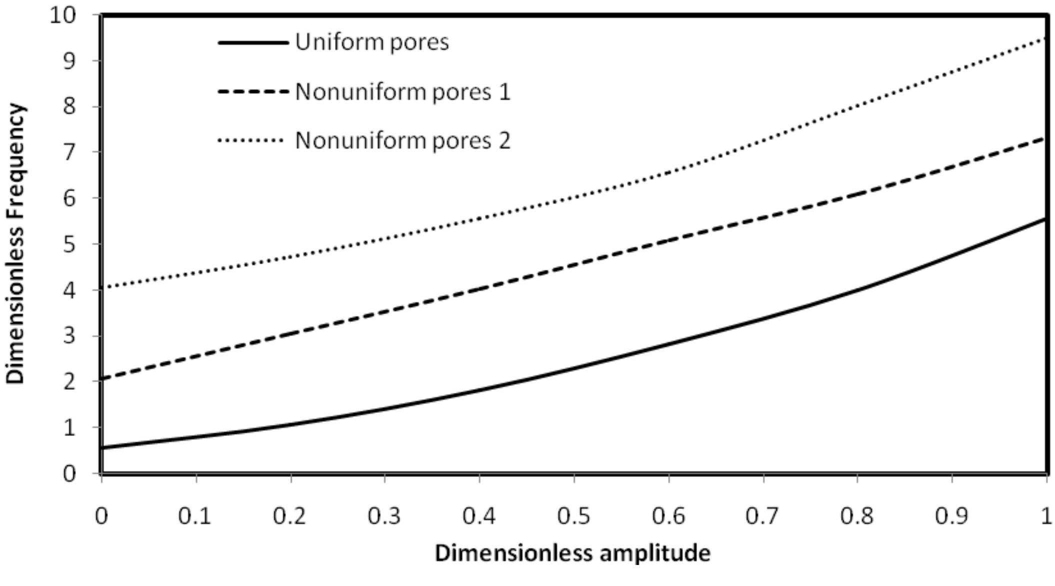

Figure 8 Changes in dimensionless frequency with dimensionless amplitude for C-C boundary.

(α,β)	$(e_0 = 0.25)$			$(e_0=0.5)$		
	M1	M2	M3	M1	M2	M3
$(0,0.5)$	4.2151	4.2403	4.3426	4.0076	4.0775	4.2511
$(0.5,0.5)$	4.8474	4.9872	4.8692	4.7112	4.8430	4.9522
$(0.5,0)$	5.5647	5.6966	5.6625	5.4685	5.4844	5.8029
$(-0.5,0)$	6.2604	6.2625	6.3683	6.1122	6.1911	6.3618
$(0,-0.5)$	6.9675	6.9685	7.0676	6.8276	6.8976	7.0225

Table 1 Comparison of dimensionless frequencies using BPs method.

(α,β)	$(e_0 = 0.25)$			$(e_0=0.5)$		
	M1	M2	M3	M1	M2	M3
$(0,0.5)$	4.2469	4.1053	4.2473	4.2469	4.2426	4.3841
$(0.5,0.5)$	4.9545	4.9501	5.0964	4.9511	4.9497	5.0927
$(0.5,0)$	5.6625	5.6556	5.8041	5.6624	5.6593	5.8041
$(-0.5,0)$	6.3693	6.2288	6.3712	6.3668	6.2257	6.5118
$(0,-0.5)$	7.0732	6.9290	7.2125	7.0680	6.9366	7.0704

Table 2 Comparison of dimensionless frequencies using OBPs method.

Frequency Parameter	$\varsigma = 0$		$\varsigma = 0.1$		$\varsigma = 0.3$	
	Present	(wang et al., 2007)	Present	(wang et al., 2007)	Present	(wang et al., 2007)
S-S boundary						
1	3.1406	3.1416	3.0683	3.0685	2.6800	2.6800
2	6.2830	6.2832	5.7814	5.7817	4.3014	4.3013
3	9.4241	9.4248	8.0400	8.0400	5.4420	5.4423
4	12.564	12.566	9.9161	9.9162	6.3630	6.3630
C-S boundary						
1	3.9264	3.9266	3.8207	3.8209	3.2828	3.2828
2	7.0685	7.0686	6.4647	6.4649	4.7664	4.7668
3	10.210	10.210	8.6515	8.6517	5.8370	5.8371
4	13.251	13.252	10.467	10.469	6.7144	6.7145
C-C boundary						
1	4.7300	4.7300	4.5945	4.5945	3.9184	3.9184
2	7.8530	7.8532	7.1401	7.1402	5.1962	5.1963
3	10.995	10.996	9.2583	9.2583	6.2314	6.2317
4	14.135	14.137	11.015	11.016	7.0482	7.0482

Table 3 First four frequency parameters of Euler-Bernoulli nanobeams for different scaling effect parameters and boundary conditions